

PHASE SPACE TOMOGRAPHY RESEARCH AT DARESBUURY*

K. M. Hock[†], M. G. Ibsion, A. Wolski, University of Liverpool and Cockcroft Institute, UK
 D. J. Holder, University of Manchester and Cockcroft Institute, UK
 B. D. Muratori, ASTeC, STFC Daresbury Laboratory and Cockcroft Institute, UK

Abstract

We report on the progress of phase space tomography research at Daresbury. The effort over the past three years has been focussed on measuring the electron beam at the ALICE tomography section. Based on the results, we have developed techniques for improving resolution using normalised phase space and for removing streaking artefacts. We have developed in-house reconstruction codes using both Filtered Back Projection and Maximum Entropy Technique. We use a combination of simulation and measurements to investigate the onset of space charge effects at over short distances. We are currently developing methods for full 4D phase space reconstruction.

INTRODUCTION

Phase space tomography is a measurement technique that is used in accelerators to characterise the phase space of a particle beam. It has been used in a number of accelerators, including PITZ [1], UMER [2], SNS, PSI [3], CERN [4], BNL [5], FLASH [6] and TRIUMF [7]. Phase space tomography measures the distributions of a beam in 2D phase spaces: (x, x') , (y, y') or (z, δ) . The standard implementation uses elements such as quadrupoles and scintillating screens, combined with a measurement procedure and computer codes to reconstruct the phase space distribution.

We report on our research on the ALICE test facility at Daresbury Laboratory. The goals of our work are as follows:

- Set up tomographic measurement in the ALICE tomography section. This is a section of the injection line that transfers the electron beam from ALICE to EMMA (the world's first non-scaling fixed-field alternating gradient accelerator).
- Carry out measurements to characterise the electron beam from ALICE which is subsequently injected into EMMA.
- Develop measurement, processing and reconstruction techniques to improve the results from phase space tomography.

In this paper, we describe the measurement setup, procedure and results. We then discuss some improvements to the techniques and our attempts to observe the effect of space charge. Finally, we summarise our efforts to develop

a method to measure and reconstruct the full 4D transverse phase space.

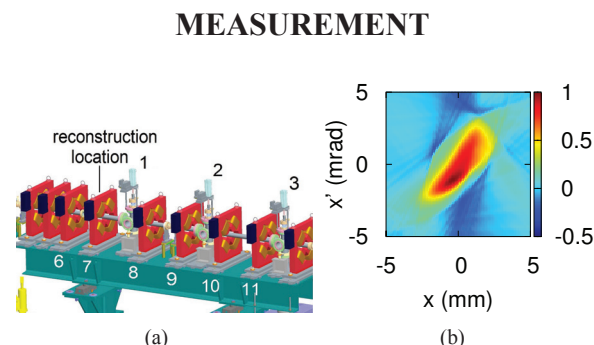


Figure 1: (a) ALICE tomography section. The electron beam is travelling from left to right. (b) Measured phase space for a 12 MeV beam with 80 pC bunches.

The ALICE tomography section is shown in Fig. 1(a). It consists of two FODO cells between three YAG screens (labelled 1-3). The distance from screen 1 to screen 3 is 1.5 m. Each quadrupole is 7 cm long, with a gradient that can be adjusted between 0 and about 15 T/m. When a bunch of electrons is incident on a screen, it produces luminescence proportional to the flux of electrons arriving at each point on the screen. The decay time of this luminescence is about 70 ns. Viewing each screen is a Pacific board camera (model PC-375) capturing 50 images per second. The ratio of distance on the screen to pixel size on a captured image is about 0.1 mm/pixel, depending on focussing setup at the screen.

In our experiments [8], we have used a 12 MeV electron beam with a repetition rate of a few Hertz. As an example, a tomographic measurement at ALICE involves varying the strength of quadrupole 7 and capturing the beam images on screen 1. The images are then transformed to projections at different angles in the (x, x') phase space at the reconstruction location at the entrance to quadrupole 7 (in Fig. 1(a)). The reconstruction location can be chosen to be anywhere, but is likely to give more reliable results if it is close to the measurement setup. The reconstruction location indicated in Fig. 1(a) is used for the results in this paper. The distribution of particles in (x, x') can then be reconstructed using a standard reconstruction algorithm, such as Filtered Back Projection (FBP) or Maximum Entropy Technique (MENT). A typical result is shown in Fig. 1(b). Using just quadrupole 7, the projection angles can be adjusted over a range of up to 160° only (the ideal range is 180°). Notice the lines radiating from the central region

* Work supported by Science and Technology Facilities Council, UK

[†] kmhock@liverpool.ac.uk

in the background in Fig. 1(b). These are clearly unphysical because they often extend in straight lines of uniform intensity up to the edges of the reconstructed image, well beyond the transverse size of the screen image. A simple way to remove these streaking artefacts would be as follows: To calculate the tomographic projection from each screen image, we impose a threshold intensity (for example 10% of the peak value) below which any signal is regarded as background and neglected. For each projection angle, this corresponds to a region in the phase space as illustrated in Fig. 2(a). By setting the reconstructed distribution in this region to zero for every angle, the streaking artefacts would be removed compare Fig. 2(a) with 1(b). It is possible that this also removes real but weak signals such as halo. So this technique should be used with caution. Simulations suggest that space charge has an effect

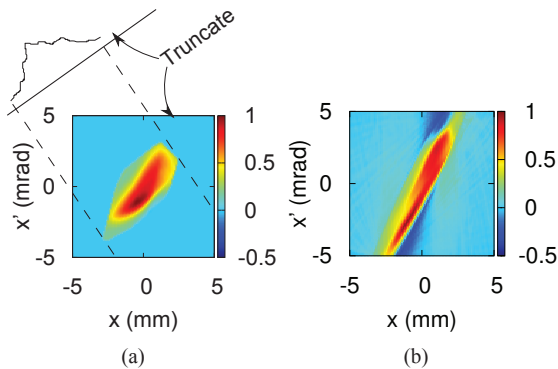


Figure 2: (a) Streaking artefacts removed from Fig. 1(b). (b) Reconstruction showing the possible effect of space charge.

on the beam size as the bunch charge is increased from 20 to 80 pC [9]. Therefore we set up a second tomographic experiment to capture the images at screen 3. We reconstruct the phase space at the same reconstruction location. The result is shown in Fig. 2(b). We would expect that the result is the same as that from the screen 1 measurement in Fig. 2(a) since they are both reconstructed at the same location. They look different. This suggests the possibility of space charge or other effects.

NORMALISED PHASE SPACE

Phase space distributions are often long and narrow because of long drift spaces. This leads to problems in sampling of the projections. The angles close to the long axis of the distribution may not be sufficiently well sampled. This will lead to a distortion of the reconstructed result. We find that this distortion can be significantly reduced by sampling at uniform angle intervals in normalised phase space (x_N, x'_N) instead of in coordinate phase space (x, x') . The two spaces are related by

$$\begin{pmatrix} x_N \\ x'_N \end{pmatrix} = \begin{pmatrix} \frac{1}{\sqrt{\beta}} & 0 \\ \frac{\alpha}{\sqrt{\beta}} & \sqrt{\beta} \end{pmatrix} \begin{pmatrix} x \\ x' \end{pmatrix} \quad (1)$$

In normalised phase space, $\beta = 1$ m and $\alpha = 0$. So a distribution tends to be more circular, and sampling at uniform intervals of angles is better suited to accurate reconstruction. One way to implement this in phase space tomography is as follows [10]:

- Measure the Twiss parameters at the reconstruction location using a quadrupole scan.
- Combine the above matrix for transformation to normalised phase space with the matrix for mapping from the reconstruction location to the screen.
- Use the standard measurement and reconstruction procedure for phase space tomography.

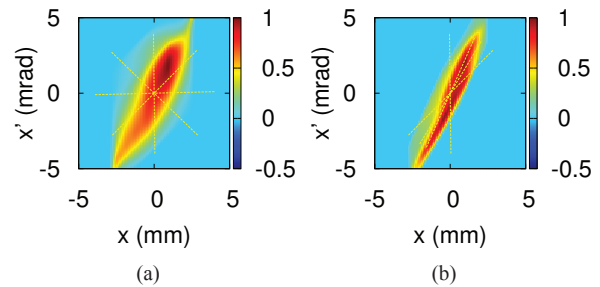


Figure 3: MENT reconstruction of Fig. 2(b) using (a) 4 angles in coordinate phase space and (b) 4 angles in normalised phase space. Yellow lines show ray directions of projections.

We have carried out simulations on a variety of hypothetical distributions [10, 11] and find that the distortions due to sampling at equal intervals in coordinate phase space can be reduced. Figure 3 shows a comparison of the results obtained from reconstructions using MENT. Using the measurement data obtained for Fig. 2(b) (which is reconstructed from 159 projections), we select four at uniform intervals of angles in phase space without normalisation and reconstruct the distribution. The result, shown in Fig. 3(a), is significantly broader than that in Fig. 2(b). In this test case, Fig. 2(b) may be considered as our original distribution - it is likely to be close to the original because of the large number of angles sampled; we could also treat it as a hypothetical distribution. We then select 4 projections at uniform angle intervals in normalised phase space from the 159 projections. As it is unlikely that we can find projections at exactly the right angles, we choose the 4 closest match. Using these 4 projections, we reconstruct the distribution using MENT again. The result shown in Fig. 3(b) is much closer to the original in Fig. 2(b). This clear improvement with so few projections demonstrates the usefulness of this technique. Each yellow line in Fig. 3(b) represents a ray direction, which is perpendicular to a projection direction [10]. Each value in a projection is obtained by integrating the distribution along one of its rays. Apart from sampling at uniform intervals, reconstructing in normalised phase space may also offer additional insights. Recall that although Fig. 1(b) and Fig. 2(b) are distributions reconstructed at the same location, they use data

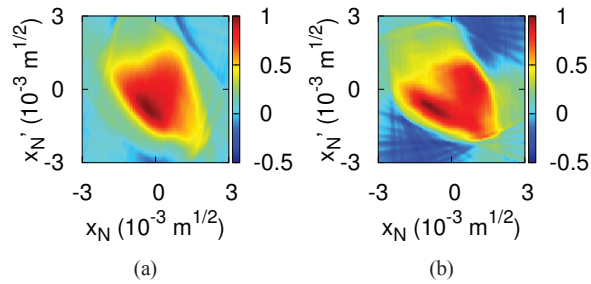


Figure 4: Reconstruction in normalised phase space for the same location just before quadrupole 7, using beam images at: (a) screen 1; (b) screen 3.

recorded at screens 1.5 m apart, and look quite different. This was thought to be due to the effect of space charge. Figure 4 shows the corresponding results reconstructed in normalised phase space. Structures that are not obvious in Figs. 1(b) and 2(b) are now clearly visible. Notice that Fig. 4(a) and (b) actually have broadly similar shapes and that one appears to be rotated with respect to the other. This is something that we cannot see in Figs. 1(b) and 2(b). A rotation in normalised phase space could arise from linear effects, possibly from space charge or magnet errors.

4D RECONSTRUCTION

We have also developed a 4D reconstruction method [12] and shown in simulations that it is feasible to carry it out at ALICE. The standard phase space tomography technique is only able to reconstruct a 2D phase space. A distribution in (x, x') phase space, for instance, is a projection of the full 6D distribution and does not contain information on correlation between other coordinates. Our method measures and reconstructs the 4D (x, x', y, y') phase space. It can be implemented using quadrupoles 6 and 7 and screen 1 shown in Fig. 1(a). From the work described in the earlier sections, we know that the focussing quadrupole 7 can rotate in (x, x') and the defocussing quadrupole 6 can rotate in (y, y') . The steps are as follows:

- For each (y, y') angle, record the screen 1 images for different (x, x') angles.
- Repeat this for different (y, y') angles.

When quadrupole 7 rotates in (x, x') , it will also rotate in (y, y') by a smaller amount. We can compensate for this by adjusting quadrupole 6 so that the net rotation in (y, y') is zero. Likewise for the rotation in (y, y') [12]. The full set of recorded images can then be processed using a series of 2D reconstructions to reconstruct the 4D phase space. The details, equations and algorithm are given in [12]. To demonstrate this technique in simulation, we have modelled a hypothetical distribution of 125000 particles in (x, x', y, y') . It is difficult to visualise a 4D phase space and so we show only the projection of this distribution on (y, x') in Fig. 5(a) for illustration. Using the parameters for quadrupoles 6 and 7 and screen 1, we simulated the screen images and measurement procedure. Although it is

possible to rotate in (x, x') using quadrupole 7, the strength of quadrupole 6 must be adjusted to keep the (y, y') angle from changing. Likewise, when we rotate in (y, y') using quadrupole 6, the strength of quadrupole 7 must be adjusted to keep the (x, x') angle fixed. Using the algorithm in [12], we can then reconstruct the full 4D phase space. A projection of this on (y, x') is shown in Fig. 5(b). It compares well with Fig. 5(a). The background is higher because our two-quadrupole setup only provides maximum angle ranges of 160° and 150° in (x, x') and (y, y') respectively.

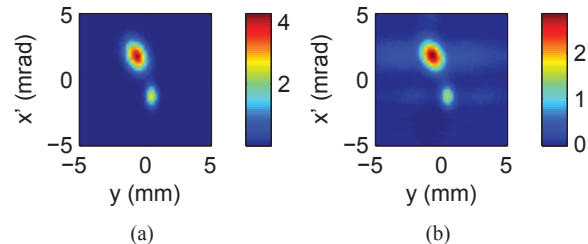


Figure 5: (a) Projection of a (x, x', y, y') distribution on (y, x') . (b) Corresponding projection of the reconstructed distribution.

ACKNOWLEDGMENT

We are grateful to Rob Smith and Ben Shepherd for their help with the measurements.

REFERENCES

- [1] S. Rimjaem, et al, "Measurements of transverse projected emittance for different bunch charges at PITZ", FEL 2010, Malmö.
- [2] D. Stratakis, et al, Phys. Rev. ST Accel. Beams 9, (2006) 122801.
- [3] D. Reggiani, et al, "Transverse phase-space beam tomography at PSI and SNS proton accelerators", IPAC 2010, Kyoto.
- [4] Phase space tomography, <http://tomograp.web.cern.ch/tomograp/>
- [5] V. Yakimenko, et al, Phys. Rev. ST Accel. Beams 6, 122801 (2003)
- [6] K. Honkavaara, et al, "Electron beam characterization at PITZ and the VUV-FEL at DESY", FEL 2005, Stanford.
- [7] Y.-N. Rao and R. Baartman, "Transverse phase space tomography in TRIUMF injection beamline", IPAC 2011, San Sebastian.
- [8] M. G. Ibson, et al, JINST, 7, P04016 (2012).
- [9] B. Muratori, et al, "Space charge effects for the erl prototype at Daresbury Laboratory", EPAC 2004, Lucerne.
- [10] K. M. Hock, et al, NIM A, 642, (2011), pp. 36-44.
- [11] K. M. Hock and M. G. Ibson, JINST, 7, P04016 (2012).
- [12] K. M. Hock and A. Wolski, "Tomographic Reconstruction of the Full 4D Transverse Phase Space", submitted to NIM A (2013).